

CURRENT RESEARCH

Formation of Hydrocarbons and Oxides of Nitrogen in Automobile Engines

John B. Heywood¹ and James C. Keck

Department of Mechanical Engineering, Massachusetts Institute of Technology, Cambridge, Mass. 02139

■ The basic mechanisms responsible for the production of nitrogen oxide and hydrocarbon emissions from automotive spark-ignition engines are reviewed. It is shown how the formation of nitric oxide is rate controlled in the high-temperature burned gases inside the engine cylinder. A mathematical model which predicts nitric oxide emissions for given engine design and operating variables is then described. In contrast, the hydrocarbons are formed when the flame quenches at the cylinder head and piston walls. The magnitude of these quench layers and crevices and the boundary layer aerodynamics by which the hydrocarbon-rich gases exit the cylinder are discussed.

In the paper we have the privilege of presenting at this symposium honoring Professor Haagen-Smit, we will review what has been learned about the basic processes responsible for the production of hydrocarbons and nitrogen oxides in automotive engines. The objective of this work has been to develop the quantitative understanding of these processes necessary for the design and evaluation of techniques for reducing smog at its source. The importance of this objective is easily appreciated when one considers the tremendous capital investment required to make even minor changes in the millions of automobiles produced annually and to monitor their performance once they are on the road. Other aspects of the problem, including the emission of particulates, the atmospheric reactions between hydrocarbons and oxides of nitrogen which produce smog, and the measures necessary to develop control programs are discussed in the subsequent papers at this symposium.

The 100 million motor vehicles on the road in the U.S. today are the source of about 60 million tons of CO, 16 million tons of HC, and 7 million tons of NO_x annually—1200 lb of CO, 320 lb of HC, and 140 lb of NO_x per car. In an uncontrolled vehicle—that is a car sold before any emission controls were required—these emissions came from the engine crankcase, from fuel evaporation in the fuel tank and carburetor, and from the exhaust. The crankcase and evaporative HC emissions are now effectively controlled in all new vehicles. The engine itself is responsible for the remaining source of HC and of CO and NO_x emissions. Though 80 and 70% control of HC and CO exhaust emissions, respectively, has already been achieved with current new vehicles, substantial further reductions in all exhaust emissions will be required within the next five years. The control techniques already employed, and those proposed for the future have been reviewed by Brehob (1971). Here we will concentrate on the physics and chemistry of pollutant formation.

The processes responsible for the production of hydrocarbons and nitrogen oxides in the cylinder of a spark-ignition engine are illustrated qualitatively in Figure 1 which

shows three important stages in the combustion process. In the first stage the compressed fuel-air mixture is ignited, and a flame front propagates across the chamber. As the flame approaches the walls, it is quenched leaving behind an extremely thin layer of unburned gas typically a few thousandths of an inch thick. Unburned gas is also left in the crevice above the piston ring between the piston and cylinder wall. This unburned gas is the source of the hydrocarbons. At the same time nitric oxide (NO) is formed in the combustion products throughout the cylinder by high-temperature nonequilibrium reactions involving the nitrogen and oxygen in the air. Another important pollutant also formed during the combustion is carbon monoxide (CO), but this is not important in smog formation and will not be discussed in detail. In the second stage the piston recedes depositing the unburned hydrocarbons in the crevice above the piston ring along the sides of the cylinder and rapidly cooling the bulk combustion products by expansion. As a result of the falling temperature, the chemical reactions which would normally remove the NO and CO become extremely slow, “freezing” the concentrations of these pollutants at levels far above those expected for equilibrium at exhaust temperatures. In the final stage the exhaust valve opens, and the polluted combustion products leave the cylinder—entraining parts of the unburned hydrocarbon layers on the walls as they go.

From this qualitative discussion it should be clear that the processes responsible for the production of nitric oxide and unburned hydrocarbons are distinctly different. The former involve primarily combustion kinetics, and the latter flame quenching and boundary layer aerodynamics. It is also known from the pioneering work of Hershey et al.

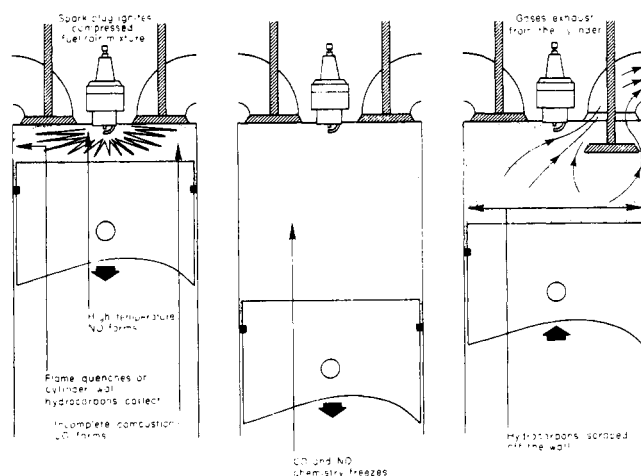


Figure 1. Schematic shows how three major pollutants—unburned hydrocarbons (HC), carbon monoxide (CO), and nitric oxide (NO)—form inside the spark-ignition engine cylinder during combustion process

¹ To whom correspondence should be addressed.

(1936) that the thermodynamic state of the burned gas in an internal combustion engine is very close to equilibrium and that the trace concentrations of pollutants present represent a minor perturbation of the system. Thus the problem of treating the production of nitric oxide and hydrocarbons may be conveniently divided into three parts: the determination of the temperature, density, and concentrations of major species for burned gas in equilibrium; the investigation of the chemical kinetics of nitric oxide in this environment; and the study of the formation and aerodynamics of the hydrocarbon-containing boundary layers.

Thermodynamics of Internal Combustion

The combustion process in a spark-ignition engine is illustrated in Figure 2. The top curve shows a typical cylinder pressure, p , vs. crank angle; the second curve, x , shows the mass fraction of the charge which has burned. The fuel-air-residual gas mixture is sparked at $\theta = -40^\circ$, and combustion is complete at about $\theta = 30^\circ$. An important consequence of the finite time required to burn the charge is the different temperature-time histories of parts of the mixture which burn at different times during the combustion process. The following model illustrates this process; more exact models are discussed later.

Based on the assumption of equilibrium in the burned gases, Lavoie et al. (1970) have developed a simple model of internal combustion which permits one to calculate the thermodynamic state of the burned and unburned gases from a knowledge of the pressure and volume of the system as a function of time. In addition to assuming equilibrium in the burned gas, the model assumes that: the original charge is homogeneous; the pressure is independent of position; the volume occupied by the gas in a state of partial combustion is negligible; the unburned gas is "frozen" at its original composition and undergoes an isentropic compression; and both burned and unburned gases have constant local specific heats. Under these conditions the mass fraction of the charge which has burned, x , can be calculated from the laws for conservation of mass and energy and the equations of state for the burned and unburned gases.

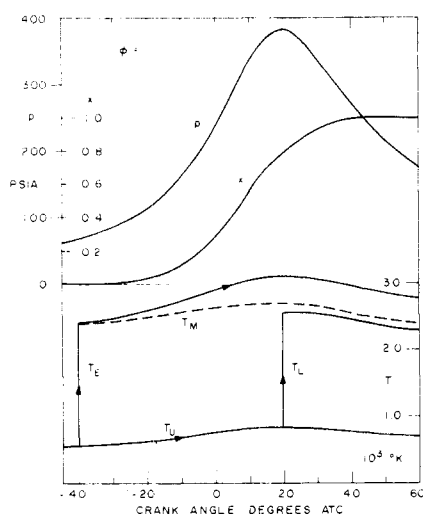


Figure 2. Gas pressure inside cylinder (p), mass fraction burned (x), and temperatures of unburned mixture (T_u) and elements of charge which burned early (T_E) and late (T_L) as a function of crank angle

Dashed line shows the average burned gas temperature (T_M) if it were fully mixed

To determine the temperature distribution in the burned gas, it is necessary to make an assumption about the state of mixing in these gases. In most previous treatments of the problem, it has been assumed that each element of the charge which burns mixes instantaneously with the previously burned gas resulting in a uniform temperature throughout the burned gases in the cylinder.

We do not believe that this "completely mixed" model is a good approximation, however, because it is incompatible with both the observations of a relatively thin turbulent flame front and substantial temperature gradients in the burned gas (Rassweiler and Withrow, 1935; Lavoie, 1970). A more realistic approximation is that there is no mixing during the early part of the combustion process, and that each element of gas which burns is isentropically compressed from its state just behind the flame front as the pressure rises. The unburned mixture is also compressed isentropically. Thus each element of the charge burns at constant but different pressure and enthalpy. Each element is then compressed and expanded isentropically as the rest of the charge burns and the piston recedes.

Typical temperature-time histories for the unmixed model are shown in the lower part of Figure 2 for two elements of gas: one which burned early in the cycle denoted T_E and one which burned later denoted T_L . Also shown are the mean temperature T_M of burned gas and the temperature T_u corresponding to isentropic compression of the unburned gas. A substantial temperature gradient exists, and the gas which burned early has a peak temperature approximately 500°K higher than that which burned late. Due to the extreme temperature sensitivity of chemical reaction rates, such temperature differences can easily produce order of magnitude variations in the concentrations of NO formed in the burned gases, and it is very important to take them into account.

For detailed kinetic calculations of the NO formation process, more accurate information on the state of the burned gases is required than can be obtained from a perfect gas model of the type described. However, the same calculation procedure can be carried out using computer programs which give the properties of the unburned mixture and the equilibrium thermodynamic properties and composition of the burned gases. Such calculations have been carried out (Heywood, et al., 1971; Blumberg and Kummer, 1971), and the magnitude of the temperature gradient across the burned gases is close to that predicted by the perfect gas model.

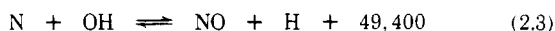
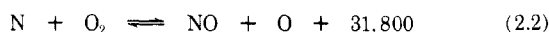
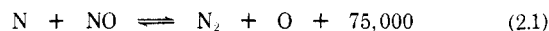
Although the "unmixed" model appears to be satisfactory for correlating measurements on actual engines where the pressure-time history can be measured, it cannot be used for design studies without the addition of a "burning law" from which pressure-time histories can be calculated. To date no satisfactory "burning law" based on fundamental principles has been developed. This gap in our knowledge is currently being bridged by the use of semiempirical "burning laws" of the type

$$x(\theta) = (1/2)[1 - \cos \pi[(\theta - \theta_o)/\Delta\theta]] \quad (1)$$

where θ_o is the apparent ignition angle which may include a substantial "ignition delay" and $\Delta\theta$ is an apparent burning angle of the order of 40-50 crank angle degrees. With $x(\theta)$ known, $p(\theta)$ can be calculated from conservation of mass and energy as described previously. There is little doubt, however, that more accurate burning laws are needed, and the deviation of these is an important area for future research.

Kinetics of NO Formation

The chemistry of NO formation in gas phase mixtures of O, N, C, and H has been extensively studied in shock tubes, stirred reactors, and flames, and rate constants for all the important reactions have been determined (see Baulch et al., 1969 for a critical review). With this work as a basis, kinetic models of NO formation in automotive engines have been proposed by Newhall and Starkman (1967), Eyzat and Guibet (1968), and Lavoie et al. (1970). Of these models, that of Lavoie et al. is most complete and includes the other two as special cases. The most important reactions to include are:



The exothermic rate constants are given in Table I. The exothermicities and activation energies are in cal/g-mol, and the rate constants are in cm^3/sec .

If we assume that the concentrations of O, O_2 , OH, H, and N_2 are in local equilibrium in the burned gases, the Reactions 2.1 to 2.3 may be combined to give two first-order nonlinear differential equations for the concentrations of NO and N. Although numerical integration of this pair of equations is possible, it can easily be shown that the characteristic relaxation time for N is several orders of magnitude shorter than that for NO. It is thus an excellent approximation to assume a steady-state value for N. The set may then be reduced to a single equation for the NO formation rate:

$$\frac{d\{\text{NO}\}}{dt} = \left(\frac{2M_{\text{NO}}}{\rho}\right)(1 - \alpha^2) \left(\frac{R_1}{1 + \alpha K}\right) \quad (3)$$

where $\{\text{NO}\}$ is the mass fraction of NO, M_{NO} is the molecular weight of NO, ρ is the gas density, $\alpha = [\text{NO}]/[\text{NO}]_e$ is the concentration of NO divided by its equilibrium value, $K = R_1/(R_2 + R_3)$, and R_i is the "one-way" equilibrium rate of the i th reaction—e.g., $R_1 = k_1[\text{NO}]_e[\text{N}]_e$. This reaction scheme corresponds to the well-known Zel'dovich mechanism extended to include the reaction of N with OH.

If Reaction 2.3 is omitted, K in Equation 3 is then R_1/R_2 . Typical values of R_1 , R_1/R_2 , and $R_1/(R_2 + R_3)$ for lean, stoichiometric, and rich mixtures are given in Table II. Since α can exceed unity under spark-ignition engine conditions, the addition of Reaction 2.3 to the Zel'dovich mechanism would be expected to affect the calculated NO concentrations especially for rich mixtures. For example,

Table I. Exothermic Rate Constants for Reactions 2.1 to 2.3

Reaction	Rate constant ^a
2.1	$5.2 \times 10^{-11} \exp(-334/RT)$
2.2	$1.1 \times 10^{-14} T \exp(-6250/RT)$
2.3	7×10^{-11}

^a Units $\text{cm}^3 \text{sec}^{-1}$. Activation energies in cal/g-mol.

Table II. Typical Values of R_1 , R_1/R_2 , and $R_1/(R_2 + R_3)$ ^a

Equivalence ratio	R_1 ^b	R_1/R_2	$R_1/(R_2 + R_3)$
0.8	5.8×10^{-5}	1.2	0.33
1.0	2.8×10^{-5}	2.5	0.26
1.2	7.6×10^{-6}	9.1	0.14

^a At 10-atm pressure and 2600°K.

^b Units $\text{g-mol cm}^{-3} \text{sec}^{-1}$.

for $\phi = 1.2$, the omission of Reaction 2.3 increases the calculated exhaust NO concentration by about 50% at typical engine-operating conditions.

If we use temperature, density, and species concentrations given by the full equilibrium thermodynamic model outlined in the previous section, Equation 3 may be integrated numerically to obtain the mass fraction of NO as a function of time for any element of burned gas. Although this procedure is not applicable in the flame front where the radical concentrations are far from equilibrium, there is both experimental and theoretical evidence that NO formation in this region is negligible compared to that in the postflame gas at gas pressures and temperatures typical of spark-ignition operation.

A comparison of the rate-limited and equilibrium NO mass fractions as a function of crank angle degrees is shown in Figure 3 for elements of gas which burn at -30° and 15°C . In both cases, the rate-controlled solutions rise from the residual concentration at a finite rate, cross the equilibrium solution, and "freeze" at levels well above the equilibrium values for exhaust conditions. Note that in the element of gas which burned early, the rate-controlled solution approaches equilibrium during the high-temperature part of the cycle but "freezes" at levels significantly below the peak. In the element which burned late, the rate-limited solution never reaches the peak equilibrium level. This is a result of the very much slower reaction rates associated with the lower temperature of the gas which burns late in the cycle.

Experimental studies of the time and space dependence of NO formation in internal combustion processes have been carried out under a wide variety of conditions and have verified virtually all the predictions of the "unmixed" model of NO formation. Using the γ -band absorption technique, Newhall and Shahed (1971) have measured the NO production as a function of time behind hydrogen/air flames in a cylindrical bomb. Their results are compared with the predictions of the "unmixed" model in Figure 4, and it can be seen that the agreement is excellent. Note that the NO concentration rises smoothly from zero indicating there is negligible production in the flame front.

The effect of the temperature gradient on NO production in single-cylinder reciprocating piston engines burn-

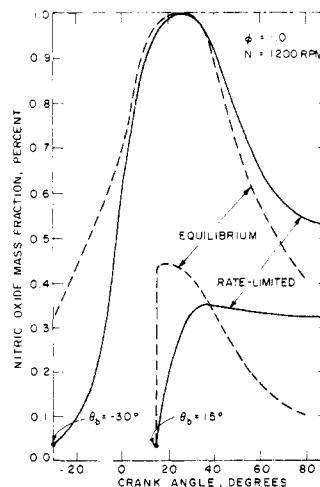


Figure 3. Calculated NO concentrations as functions of crank angle in two elements which burn at different times (-30° and 15°)

Dashed lines are NO mass fraction if NO were in equilibrium; solid lines are rate-limited NO concentrations

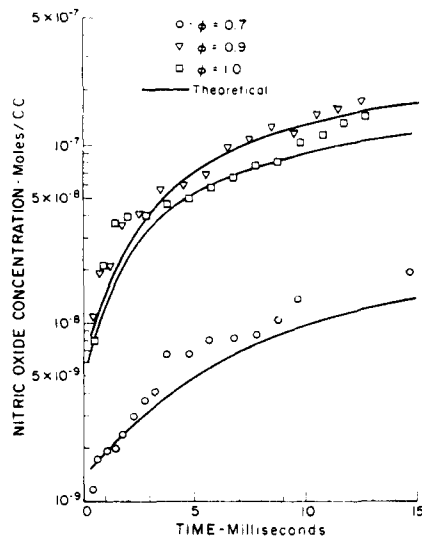


Figure 4. Measured and calculated rate-limited NO concentrations behind flame in high pressure cylindrical bomb experiments by Newhall and Shahed (1971) with lean and stoichiometric hydrogen-air mixtures. An "unmixed" model was used for the calculations—i.e., each element of mixture retained its identity after combustion

ing hydrocarbon/air mixtures has been demonstrated by Alperstein and Bradow (1967) and Starkman et al. (1969) using gas-sampling techniques, and by Lavoie (1970) using the chemiluminescent radiation from the reaction $\text{NO} + \text{O} \rightarrow \text{NO}_2 + \text{hv}$. The measurements of Lavoie are compared with the predictions of the "unmixed" model in Figure 5 which shows the NO mole fraction at two distances from the spark plug as a function of crank angle. The stars indicate the estimated NO concentration due to mixing of the residual gas with the fresh charge. NO levels observed at window W_2 closest to the spark were substantially higher than those observed at window W_3 . The effect of the residual gas was not included in calculating the kinetic solutions, and the NO concentration ahead of the flame front was assumed to be zero. This has little effect on the frozen NO concentrations, and the agreement between theory and experiment is satisfactory.

The unmixed model may also be used to calculate the average NO mass fraction in the exhaust of automotive engines. This requires an evaluation of the integral

$$\{\overline{\text{NO}}\} = \int_0^1 \{\text{NO}\}_f dx \quad (4)$$

where $\{\text{NO}\}_f$ is the final frozen NO mass fraction in the element of charge which burned when the total mass fraction burned was x . The predictions of the model have been compared with the results of numerous experimental investigations by Blumberg and Kummer (1971). In general, they report good agreement between the calculated and measured exhaust NO concentrations over a wide range of engine-operating conditions.

An example of our own comparisons between measured and calculated exhaust NO concentrations in single-cylinder CFR experiments is shown in Figure 6. Measured pressure-time curves were used to generate burned gas temperatures and species composition using the "unmixed" thermodynamic model. Equations 3 and 4 were then used to obtain exhaust NO concentrations. The agreement is within the experimental error and uncertainties in the calculation procedure over a wide range of fuel-air ratios.

Blumberg and Kummer have also shown that the "unmixed" model may be used as an effective design tool to evaluate various practical methods of reducing exhaust NO emissions. This technique is illustrated in Figure 7 which shows the effect of recycling various fractions of the exhaust on the NO emissions. It can be seen that, for a given total mass of gas, NO can be more effectively reduced by recirculating exhaust gas than by adding excess air. This is due in part to the higher heat capacity of the exhaust gas which makes it more effective than air in reducing the peak burned gas temperatures, and in part to the oxygen in the air which favors the formation of NO.

Origin of Unburned Hydrocarbons

The variation of engine HC emissions with air-fuel ratio provides a starting point for this discussion. Emissions are

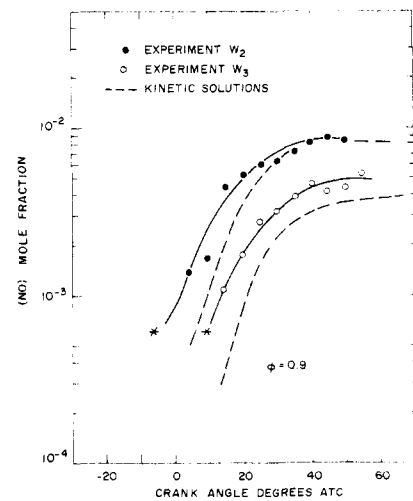


Figure 5. Measured and calculated NO concentrations in single-cylinder CFR engine experiments of Lavoie (1970). NO concentrations were measured by monitoring radiation from burned gases through quartz windows in cylinder head. Flame front reaches window W_2 earlier (-5°) than window W_3 (10°), and a higher final NO concentration is measured and predicted at W_2

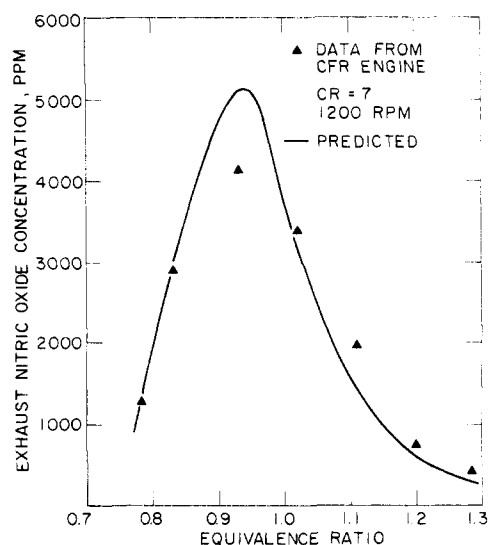


Figure 6. Comparison of measured exhaust NO concentrations in one of our single-cylinder CFR engines, with predictions made using measured pressure-time curves, the "unmixed" thermodynamic model, and rate-limited NO formation calculations. Compression ratio 7.0, engine speed 1200 rpm, spark advance 30° BTC, wide-open throttle

higher for both fuel-rich and fuel-lean mixtures with minimum emissions occurring at an air-fuel ratio of about 18:1. The rise in emissions as the mixture becomes very lean is due to engine misfire. The flame does not propagate across the charge fast enough to complete combustion before the expansion process cools the gases and quenches the flame reactions. Under normal engine operation, combustion is essentially complete in the bulk of the gas. It is the quench layers and crevices at the cylinder walls, as outlined at the beginning, which are the source of the unburned hydrocarbon.

Figure 8 shows schematically how these hydrocarbon-rich regions are formed. Daniel (1957) was the first to demonstrate the existence of quench layers with photographs showing a decrease in flame luminosity close to the wall. The flame propagates up to the wall, but heat transfer from the unburned mixture adjacent to the cool cylinder wall and piston face quenches the flame reactions before the last few thousandths of an inch of mixture is fully burned. Hydrocarbon compounds formed by heating, but not completely burning the fuel, and the gasoline hydrocarbon components are left in these layers. Over 200 organic compounds have been identified by gas chromatographic analysis of the exhaust.

The thickness of the quench layer q_d depends on the pressure p and temperature T_u of the unburned mixture at the time quenching occurs and on the fuel-air ratio.

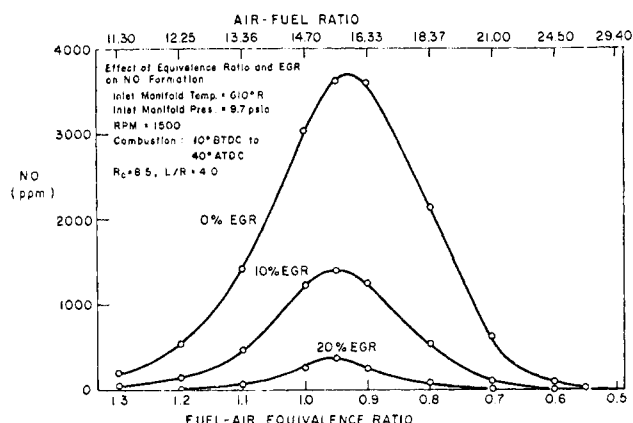


Figure 7. Results of calculations of exhaust NO concentrations for a range of exhaust gas recycle fractions and equivalence ratios by Blumberg and Kummer (1971)

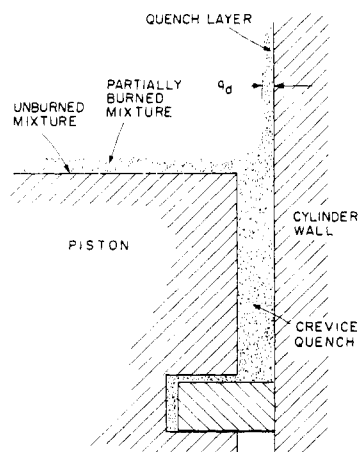


Figure 8. Schematic section of part of the piston and cylinder wall showing quench layers and the piston crown-first ring-cylinder wall quench volume

Measurements of quench distances on plane walls have been correlated with these variables as

$$q_d = q_r (\rho_r / \rho)^\alpha (T_r / T_u)^\beta \quad (5)$$

where subscript r denotes a reference condition. Examples of values of q_r , α , and β estimated by Daniel (1970) are given in Table III. It is seen that q_r is least for rich mixtures as expected since flame speeds are greatest. Typical values of q_d measured by Daniel (1957) in an engine at about stoichiometric fuel-air ratios increase from 0.003 in. at full throttle to 0.015 in. at idle. Since the flame reaches different parts of the cylinder wall at different times, quench distances are not uniform over the cylinder head and piston face.

A further source of unburned hydrocarbons are crevices in the combustion chamber which are too narrow for the flame to enter. The most important crevice is the volume between the piston and cylinder wall above the first piston ring shown in Figure 8. The flame is quenched by wall cooling at the crevice entrance. Other quench crevices around the valves and between piston face and cylinder head have now been largely eliminated.

The mass of HC formed in quench crevices, m_{qc} , is given by

$$m_{qc} = V_{qc} F \rho_u(p, T_u) / (1 + F) \quad (6)$$

where V_{qc} is the quench crevice volume, F is the fuel:air ratio, and ρ_u is the fuel-air mixture density at the pressure and temperature at which flame quenching at crevice entrance occurs. The relative importance of the piston crown-cylinder wall crevice is indicated by results of Wentworth (1969); a reduction in this crevice volume by 80% reduced exhaust HC by 40%.

The aerodynamics of these dense hydrocarbon-rich quench gas layers adjacent to the wall during the expansion and exhaust strokes will determine what fraction of the total HC formed during each cycle will be exhausted. In addition, some of the unburned HC which mixes with the bulk burned gas will be oxidized, the amount varying with fuel-air ratio and gas temperature. One would therefore expect the HC concentration in the gas leaving the exhaust valve to be nonuniform.

Daniel and Wentworth (1964) were the first to show such nonuniformities exist; Figure 9 shows HC concentrations they measured in the engine exhaust port with a rapid-acting sampling valve. High concentrations were measured at the end of the exhaust stroke; the early part of the exhaust stroke cannot be resolved, however, because the fresh exhaust mixes with gas left in the exhaust port from the exhaust process in the previous cycle. To link exhaust HC measurements such as these with the quench layers and crevices which form while the piston is close to top dead center, the flow inside the cylinder and out of the exhaust during the expansion and exhaust strokes must be understood.

Table III. Typical Parameter Values in Quench Distance Correlation^a

Air-fuel ratio	r_{r3} in 10^{-3}	α	β
20:1	5.8	0.55	0.89
14.7:1	3.1	0.52	0.56
12.6:1	2.7	0.66	0.71

^a $q_d = q_r (\rho_r / \rho)^\alpha (T_r / T)^\beta$. Values given are for $p_r = 287$ psia, $T_r = 540^\circ R$ (from Daniel, 1970).

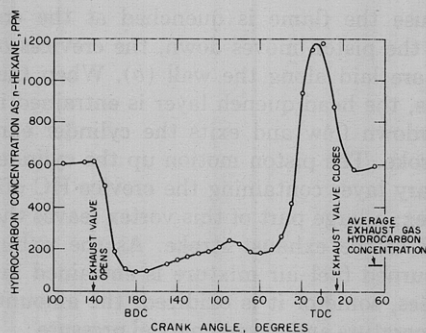


Figure 9. Hydrocarbon concentrations measured by Daniel and Wentworth (1964) with a rapid-acting sampling valve in the exhaust port during the exhaust stroke in a single-cylinder engine

Tabaczynski et al. (1972) have shown what happens to the gas in the piston crown cylinder wall crevice. As the piston moves down the expansion stroke, this gas expands out of the crevice and is laid along the cylinder wall. As the piston moves up during the exhaust stroke, the boundary layer on the cylinder wall (which contains these hydrocarbons) is scraped off the wall and rolled into a vortex. Figure 10 shows a photograph taken of a hydraulic analog of this flow. The schematic underneath indicates the geometry; the piston is the vertical surface at the left, and it scrapes the boundary layer shear flow which appears dark in the photograph, into a vortex. Tabaczynski et al. (1970) have shown that the area of this vortex divided by the square of the stroke correlates with the Reynolds number.

Tabaczynski et al. (1972) also made measurements of the mass flow rate out of the exhaust valve and the hydrocarbon concentration in the gas in the exhaust port as functions of time. They were able, therefore, to calculate the HC mass flow rate as a function of time and provide additional data to support these aerodynamic models of how the unburned hydrocarbons exit the cylinder.

Figure 11 shows the instantaneous mass flow rate out of the exhaust valve. During the first part of the blowdown process, the flow is choked; as the cylinder pressure falls, the mass flow rate decreases until the flow due to piston motion becomes important. The earlier solid line represents an isentropic compressible flow analysis treating the valve as a nozzle; the second solid line assumes the burned gases are incompressible and are pushed out of the valve by the piston. Both models are good approximations to the measured flow in the regions where they should apply.

Measured HC concentrations in the exhaust port and HC mass flow rates out of the valve are given in Figure 12. A purge was used to clear the exhaust port at the end of each exhaust stroke; the HC concentration at the beginning of the exhaust stroke could then be resolved. The HC mass flow rate curve is the HC concentration curve times the exhaust mass flow rate in Figure 11; the HC mass emission during the last 60 degrees of the exhaust stroke was measured directly. The HC concentration at the end of the stroke is much higher than at the beginning, and the shape of the curve is estimated.

These measurements show that the unburned hydrocarbons exit the cylinder in two distinct peaks: one at the beginning of the exhaust stroke—during the blowdown process, and one at the end of the stroke. About half the total mass emissions come from each peak. The first peak is assumed to result from entrainment of the cylinder head quench layer during the blowdown process. The sec-

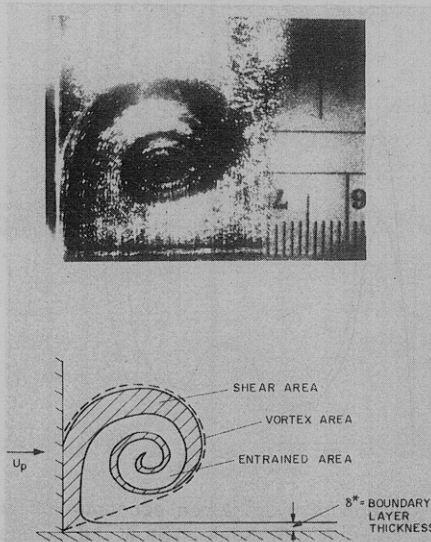


Figure 10. Photograph and schematic of vortex formed as piston (vertical surface on left) scrapes the shear layer (appears dark) off the cylinder wall in hydraulic analog experiments of Tabaczynski et al. (1970)

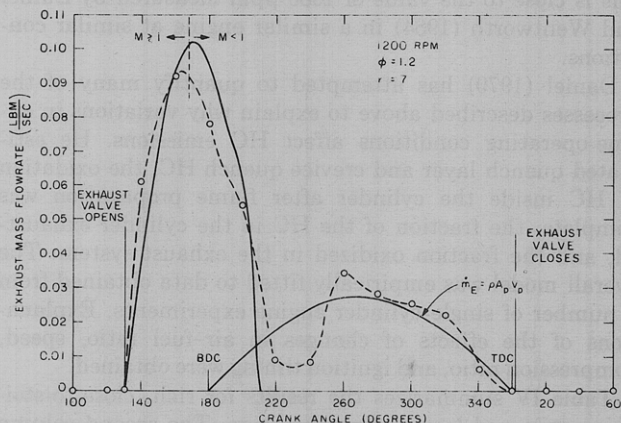


Figure 11. Measured instantaneous mass flow rate (dashed line) out of the exhaust valve of a single-cylinder CFR engine at 1200 rpm, $\phi = 1.2$, and $CR = 7$

Solid lines show an isentropic compressible flow model treating the valve as a nozzle for the blowdown process and an incompressible model showing how the piston pushes the burned gas out of the valve during the latter half of the exhaust stroke (Tabaczynski et al., 1972)

ond peak results from the vortex motion set up by the piston scraping the hydrocarbons from the piston crown—first ring quench crevice off the cylinder wall.

Considerable evidence supports this latter phenomenon. Wentworth's (1969) data showed that an 80% reduction in this quench crevice volume gave a 40% reduction in total HC emissions, implying that about half the total HC came from the quench crevice. Tabaczynski et al. (1972) showed that the vortex in their CFR engine experiments reached the valve when the piston was about 2 in. from the cylinder head; since the clearance height is 0.75 in., a substantial portion of the vortex would be expected to exit the cylinder. If all the HC in the piston crown—first crevice is entrained in the vortex, the mass of HC would be 1.4×10^{-6} lb. The mass leaving the cylinder during the latter part of the exhaust stroke was 1.2×10^{-6} lb so 2×10^{-7} lb of the vortex HC was left inside. The clearance volume of the CFR engine is 6.3 in.³, giving a residual HC concentration after valve close of about 800 ppm from the

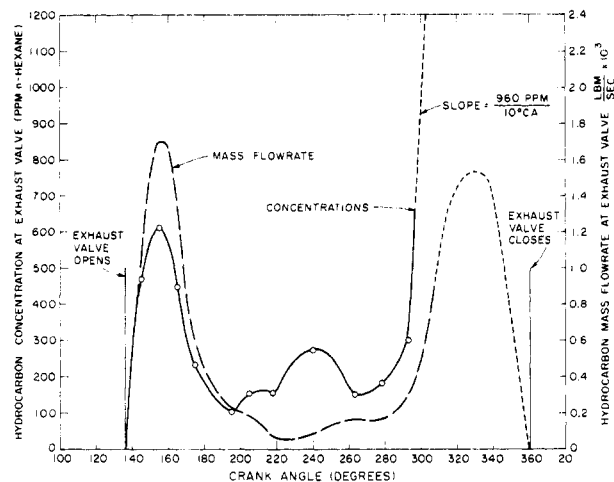


Figure 12. Variation of hydrocarbon concentration and hydrocarbon mass flow rate with crank angle at the exhaust valve of a single-cylinder CFR engine at 1200 rpm, $\phi = 1.2$, CR = 7.0 (Tabaczynski et al., 1972)

vortex. When allowance is made for the piston face quench layer, also expected to remain inside the cylinder, this is close to the value of 1085 ppm measured by Daniel and Wentworth (1964) in a similar engine at similar conditions.

Daniel (1970) has attempted to quantify many of the processes described above to explain why variations in engine-operating conditions affect HC emissions. He estimated quench layer and crevice quench HC, the oxidation of HC inside the cylinder after flame propagation was complete, the fraction of the HC in the cylinder exhausted, and the fraction oxidized in the exhaust system. The overall model was empirically fitted to data obtained from a number of single-cylinder engine experiments. Explanations of the effects of changes in air-fuel ratio, speed, compression ratio, and ignition timing were obtained.

Table IV summarizes the results for rich, close-to-stoichiometric and lean engine operation. The second column gives the exhaust HC concentration—highest for rich and lowest for lean mixtures. The ratio of quench layer HC to crevice HC is lowest for rich mixtures (because quench layers are thinnest and fuel fraction in the crevices greatest), and the proportions reverse at very lean air-fuel ratios. Little oxidation of the HC occurs subsequent to flame quenching for rich mixtures, but substantial oxidation occurs for lean mixtures. As a consequence, the HC emissions are lowest at lean air-fuel ratios until misfire occurs.

A summary of the mechanisms responsible for HC emissions is given in Figure 13. Quench layers are formed on the cylinder head, walls, and piston face as shown in (a). The crevice between piston crown and cylinder wall above the first ring is filled with fuel-air mixture at about the peak pressure and temperature; this mixture does not

burn because the flame is quenched at the crevice entrance. As the piston moves down, the crevices of HC expand and are laid along the wall (b). When the exhaust valve opens, the head quench layer is entrained in the exhaust blowdown flow and exits the cylinder early in the exhaust stroke. The piston motion up the cylinder scrapes the boundary layer containing the crevice HC off the wall into a vortex; a large part of this vortex leaves the exhaust at the end of the exhaust stroke. As the unburned and partially burned fuel-air mixture is entrained in the bulk burned gases, some of it is oxidized, the amount depending on temperature and oxygen partial pressure.

Conclusions

From this discussion it is clear that the basic mechanisms responsible for exhaust NO_x and HC emissions in reciprocating spark-ignition engines are now understood. For NO_x emissions, quantitative models give good agreement with experimental data and are already being used as design aids for lower emissions. For HC emissions, the important processes have been demonstrated, and a more complete overall quantitative model is the appropriate next stage. Though it now appears that catalysts may be required to reduce exhaust emissions to the levels required in the 1970 Clean Air Amendments, the importance of understanding the origin of the basic engine emissions will not diminish. For any reasonable expectation of meeting these requirements, the emissions from engine itself must still be held as low as is compatible with adequate engine performance. A quantitative understanding of the basic processes responsible for the production of these emissions can greatly assist in this task.

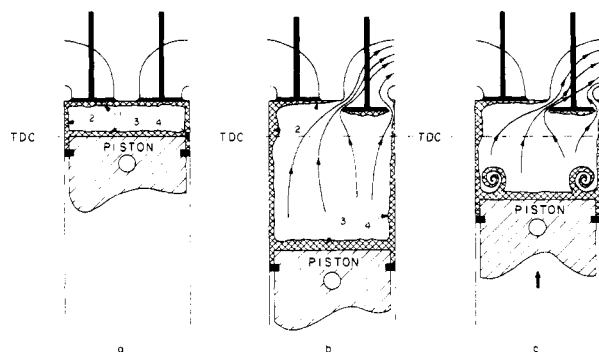


Figure 13. Schematic summarizing processes important in hydrocarbon emissions

(a) Formation of quench layers 1, 2, 3 and crevice quench 4 as flame is extinguished at cool walls. Not to scale, quench layers are about 0.003 in. thick

(b) Gas in quench volume between piston crown and cylinder wall above the first ring, 4, expands as cylinder pressure falls and is laid along cylinder walls. When exhaust valve opens, head quench layers 1 and 2 exit cylinder

(c) Roll-up of hydrocarbon rich cylinder wall boundary layer into a vortex as piston moves up cylinder during exhaust stroke

Table IV. Origin of Hydrocarbon Emissions: Rich and Lean Engine Operation^a

Air-fuel ratio	Exhaust HC, ppm	% HC from		% HC reacted in cylinder	% Unreacted HC entering exhaust	% HC reacting in exhaust	% HC entering atm
		Quench	Crevice				
12.6	680	39	61	12	55	3	47
15.7	425	44	56	38	55	10	31
20.1	320	59	41	38	55	26	26

^a From Daniel (1970).

Literature Cited

- Alperstein, M., Bradow, R. L., *SAE Trans.*, 75, paper 660781 (1967).
- Baulch, D. L., Drysdale, D. D., Horne, D. G., Lloyd, A. C., "Critical Evaluation of Rate Data for Homogeneous, Gas Phase Reactions of Interest in High-Temperature Systems," Rept. No. 4, Dept. of Physical Chemistry, Leeds University, U.K., December 1969.
- Blumberg, P., Kummer, J. T., *Combust. Sci. Technol.*, 4, 73-96 (1971).
- Brehob, W. M., SAE Repr., No. 710483 SP-365, "Engineering Know-How in Engine Design," Part 19, 1971.
- Daniel, W. A., "6th Symposium (International) on Combustion," p 886, Reinhold, New York, N.Y., 1957.
- Daniel, W. A., SAE paper 700108, SAE Automotive Congress, Detroit, Mich., January 1970.
- Daniel, W. A., Wentworth, J. T., SAE Technical Progress Ser. No. 6, "Vehicle Emissions," SAE, New York, N.Y., 1964.
- Eyzat, P. Guibet, J. C., *SAE Trans.*, 77, paper 680124 (1968).
- Hershey, A., Eberhardt, J., Hottell, H., *SAE J.*, 39, 409 (1936).
- Heywood, J. B., Mathews, S. M., Owen, B., SAE paper 710011, SAE Automotive Congress, Detroit, Mich., January 1971.
- Lavoie, G. A., *Combust. Flame*, 15, 97-108 (1970).
- Lavoie, G. A., Heywood, J. B., Keck, J. C., *Combust. Sci. Technol.*, 1, 313-26 (1970).
- Newhall, H. K., Shahed, S. M., Thirteenth Symposium (International) on Combustion, pp 381-90, The Combustion Institute, 1971.
- Newhall, H. K., Starkman, E. S., *SAE Trans.*, 76, paper 670122 (1967).
- Rassweiler, G. M., Withrow, L., *ibid.*, 125-33 (1935).
- Starkman, E. S., Stewart, H. E., Zvonow, V. A., SAE paper 690020, SAE Automotive Congress, Detroit, Mich., January 1969.
- Tabaczynski, R. J., Heywood, J. B., Keck, J. C., SAE paper 720112, *ibid.*, January 1972.
- Tabaczynski, R. J., Hoult, D. P., Keck, J. C., *J. Fluid Mechan.*, 42, 249-55 (1970).
- Wentworth, J. T., *SAE Trans.*, 77, paper 680109 (1969).

Received for review May 3, 1972. Accepted November 13, 1972. Presented at the Symposium on Science in the Control of Smog, California Institute of Technology, Pasadena, Calif., November 1971. Our own work in these areas has been supported by a number of agencies and sponsors including the Environmental Protection Agency (Grant No. 5, RO1 APO1228-02 APC), the Ford Motor Co., the MIT Sloan Basic Research Fund, the National Science Foundation (Grant No. GK15409), the Shell Co.'s Foundation Grant to the Mechanical Engineering Department at MIT, and Thermo Electron Engineering Corp.

Characterization of Particulate Matter in Vehicle Exhaust

Kamran Habibi

Petroleum Laboratory, E. I. du Pont de Nemours & Co., Inc., Wilmington, Del. 19898

■ The particulate matter emitted from present-day cars is a complex mixture of inorganic salts, soot and carbonaceous material. Measurement and characterization of such particles require elaborate sampling systems and sophisticated analytical techniques. This paper is a review of the major contributions in this area. A number of systems suitable for sampling and characterization of the exhaust particles are described. Also included is a wide selection of data from a number of workers that, in the author's opinion, best represent the state of the art.

Although the subject of vehicle emissions has received much attention during the past 15 years, there is little information on the mechanism of particle formation during engine combustion and on the character of the particles in vehicle exhaust. The main reason for this lack of information is the complexity of the physical and chemical reactions that govern particle formation and their subsequent deposition and regeneration in the exhaust system of cars. Consequently, in this area, a coherent theory can follow only in the wake of experiments, and development of proper sampling procedures and analytical techniques for characterization of exhaust particles is of great importance. Individual improvements in the techniques, no matter how small, can play a significant role in improving our understanding of the phenomenon of particulate emissions from cars.

The particulate matter emitted from present-day cars is a complex mixture of lead salts, iron as rust, base metals, soot, carbonaceous material, and tars. Measurement and characterization of these particles require elaborate sampling procedures and sophisticated analytical methods. Many factors, in particular the mode of vehicle operation, the age and mileage of the car and the type of fuel, can affect the composition and the total particulate emission rate.

Some of the particulate matter found in the exhaust is generated in the engine combustion chamber and nucleated and agglomerated in the vehicle exhaust system before it is emitted from the tail pipe. On the other hand, some of the particulate material deposits on the various surfaces of the exhaust system. At some later time, this deposited material flakes off and becomes re-entrained in the exhaust gas prior to emission from the tail pipe. Thus, during vehicle operation various types of physical and chemical processes affect the exhaust particles continuously and, as the result, the overall particulate emission process for a car is quite complex and difficult to define.

Under certain driving conditions, lead salts account for the major portion of the exhaust particles. In view of this, and for reasons relating to toxic properties of lead, most of the major studies on the exhaust particles have concentrated on characterization of the lead salts. Information on lead emission rates, chemical composition of lead-bearing particles, their size and air suspendability, and their effect on ambient air quality were considered of great importance and have been studied. This interest is reflected in the bulk of information on lead particles presented in this paper. Studies of the total particulate matter in vehicle exhaust are relatively new. The relationship of lead salts to the total particulate matter in vehicle exhaust has been considered only recently.

Early workers in the area of exhaust particles concentrated on characterization of the lead particle. Hirschler et al. (1957) carried out a comprehensive study in which the entire exhaust stream was first diluted with filtered air and then passed through an electrostatic precipitator for particle collection. The efficiency of the electrostatic precipitator was measured to be 90-95% by sampling of the effluent stream for lead concentration. The material in this effluent stream was measured and taken into account in all test runs. Hirschler coated the surfaces of the electrostatic precipitator with a polyvinyl acetate plastic,